Dalton Transactions

Cite this: *Dalton Trans.*, 2011, **40**, 3097

www.rsc.org/dalton

PERSPECTIVE

Exciton coupling in coordination compounds

Shane G. Telfer,* Tracey M. McLean and Mark R. Waterland

Received 14th September 2010, Accepted 11th November 2010
DOI: 10.1039/c0dt01226b

This Perspective reviews the impact of exciton coupling on the spectroscopic properties of coordination compounds. Exciton coupling features arise in electronic absorption and circular dichroism spectra when chromophores are brought into close spatial proximity, for example by coordination to a metal centre. The analysis of these features can reveal much information such as the geometry of a complex and its absolute configuration. The extension of the exciton coupling model to polynuclear metallosupramolecular arrays is discussed.

MacDiarmid Institute for Advanced Materials and Nanotechnology, Institute of Fundamental Sciences, Massey University, Palmerston North, New Zealand. E-mail: s.telfer@massey.ac.nz

Introduction

Electronic absorption spectroscopy is one of the foremost methods employed to characterise transition metal complexes, and circular dichroism (CD) spectroscopy occupies a similarly prominent

Tracey McLean, Shane Telfer and Mark Waterland

Shane Telfer (centre) was born in the town of Clyde in Central Otago, New Zealand. He completed a BSc(Hons) and a PhD in Chemistry at the University of Canterbury, and is now a Senior Lecturer in Chemistry at Massey University. This gradual drift northwards was punctuated by a post-doctoral odyssey that included stops in Geneva, Tokyo and Montreal. His research interests encompass synthetic inorganic chemistry and stereochemistry, with a current focus on chromophoric complexes of dipyrrin ligands and certain niche aspects of metal–organic frameworks. When not in the lab, Shane is probably in Japan.

Tracey McLean (left) gained her BSc in Chemistry and Animal Science at Massey University in 2006, followed by a BSc with first class honours in Chemistry in 2007. In 2008, she commenced study towards a PhD, which has a focus on the synthesis and spectroscopy of complexes of dipyrrin ligands. When not in the lab, Tracey is probably milking cows on her family dairy farm in Northland.

Mark Waterland (right) is currently a Senior Lecturer in the Institute of Fundamental Sciences at Massey University. He completed his BSc(Hons) and PhD degrees at the University of Otago focusing on the photophysics of transition metal complexes. His research interests centre on the use of resonance Raman spectroscopy and computational chemistry to probe the Franck–Condon dynamics of transition metal complexes, organic charge-transfer complexes, and small inorganic molecules. He is currently the President of the New Zealand Institute of Chemistry. When not in the lab, Mark is probably out riding his bike (uphill, very quickly).

position with respect to chiral complexes. The reasoned interpretation of absorption and CD spectra can provide valuable – and often unique – information regarding the composition, structure and electronic properties of coordination compounds. Models of varying sophistication can be used to interpret these spectra. The simplest approach usually involves the assignment of absorption bands to either d–d, charge transfer or ligand-centred electronic transitions. At the other end of the spectrum, a comprehensive treatment by state-of-the-art computational techniques provides a detailed picture of the electronic states of the complex and the transitions between them. The focus of this Perspective is the distinct spectral features in absorption and CD spectra that arise when two or more chromophores are brought together into close spatial proximity. These spectral features can often be interpreted within the framework of a simple model to obtain information on the complex that can be difficult or impossible to acquire *via* other means.

Exciton coupling: the essentials

A molecule may be promoted from its ground electronic state to an excited electronic state by the absorption of a photon with a wavelength that matches the energy gap between these states. The classical picture of this electronic transition involves the oscillating displacement of an electron. The spatial distribution of electron density in the excited state thus differs from that in the ground state. This creates an instantaneous dipole, termed the electric transition dipole moment (μ), which is described by a vector with an orientation corresponding to the direction of electron displacement and a magnitude that is proportional to the intensity of the transition. By way of example, the lowest energy π–π* transition in 1,10-phenanthroline (phen) has a transition dipole moment oriented as shown in Fig. 1. This electronic transition is said to be *polarised* along the long axis of the ligand.

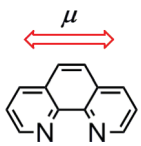

Fig. 1 The electric transition dipole for the long-axis polarised π–π* transition in 1,10-phenanthroline.

If multiple chromophores are located in close spatial proximity, the electronic excitation is no longer confined to one chromophore but becomes delocalised over the entire chromophore array. This phenomenon is termed *exciton coupling*. The term *molecular exciton* was defined by Kasha to conceptualise electronic states that involve the excitation of an assembly of molecules in concert rather than the localised excitation of individual species of the assembly.[1] The original excited states of the chromophores are *coupled* to one another to give resultant *excitonic states*.[2] It is useful to note that this does not imply that there is electron exchange between the chromophores, but rather that the excitation energy is shared between them.

In the simplest case of exciton coupling, a pair of degenerate chromophores interacts to give a set of two nondegenerate excited states. These excitonic states are linear combinations of the unperturbed excited state of the individual chromophores. One excitonic state lies at higher energy than the original excited state, while the other lies at lower energy.

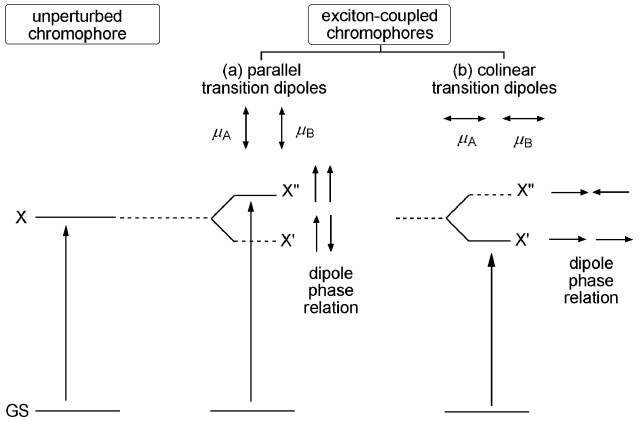

Fig. 2 Non-degenerate excitonic states (X″ and X′) are produced by the exciton coupling of spatially proximate chromophores. This is exemplified for (a) a pair of chromophores with parallel transition dipole moments; and (b) a pair with collinear transition dipole moments. Vertical arrows denote allowed transitions.

Two chromophore orientations are presented in Fig. 2, which have (a) parallel and (b) co-linear transition dipoles. An intuitive picture of the excitonic states in these two cases relies on the phase relationships between the transition dipoles of the two chromophores and was concisely summarised by Schellman:[3]

A single transition moment is represented by a double-headed arrow which indicates its oscillatory nature. When two transition moments are coupled, their relative motions become important, and the combined system is best represented by pairs of single-headed arrows which indicate the relative phases of motion. The only possibilities for two transition moments are "in phase" and "out of phase".

On electrostatic grounds, these will result in higher- and lower-energy excited states (X″ and X′), respectively. The net length of the summed vectors is proportional to the integrated band area of the electronic transitions to these excitonic states. For parallel transition dipoles (Fig. 2a), the X′ state has a zero net transition dipole hence transitions to this state are forbidden. The transition to the X″ state has a dipole with a length twice that of the individual chromophores. The net effect of exciton coupling on the electronic absorption spectrum in this case is thus to *blue-shift* the observed absorption band from that of an unperturbed chromophore. The integrated area of this band will be twice that of a single chromophore. This is a general sum rule: the net intensity of the absorption bands of the individual chromophores is exactly retained.

Two nondegenerate excited states will also result if the transition dipoles are co-linear (Fig. 2b). In this case, the head-to-tail coupling of the transition dipole vectors has a nonzero magnitude and excitation to the lower energy (X′) exciton state is allowed. Exciton coupling will be manifest by a *red-shift* of the absorption band with respect to uncoupled chromophores.

In many cases, particularly those involving transition metal complexes, the dipole moments of two interacting chromophores will not be perfectly positioned in either a parallel or co-linear arrangement. Using a system with two electronic excitations as

an example, the excitonic energy levels are most conveniently obtained as the eigenvalues of a 2 x 2 Hamiltonian

$$H = \begin{pmatrix} H_1 & J \\ J & H_2 \end{pmatrix} \quad (1)$$

H_1 and H_2 are the zeroth-order excited-state energies of the uncoupled system. The excited-states interact *via* dipolar coupling. The coupling strength, J, is determined by the electric field of the first dipole moment oriented along the z-axis, centred at $z = 0$, interacting with the second dipole centred at distance r (Fig. 3a),

$$J = E_{X''} - E_{X'} = -\mu_B \cdot E_A \quad (2)$$

where the electric field of the first dipole (E_A) is

$$E_A = \frac{1}{4\pi\varepsilon_0}\frac{1}{r^3}(3(\mu_A \cdot \hat{r})\hat{r} - \mu_A \quad (3)$$

and the strength of coupling is given by

$$J = \frac{\mu_A \cdot \mu_B}{r^3} - 3\frac{(\mu_A \cdot \hat{r})(\mu_B \cdot \hat{r})}{r^5} \quad (4)$$

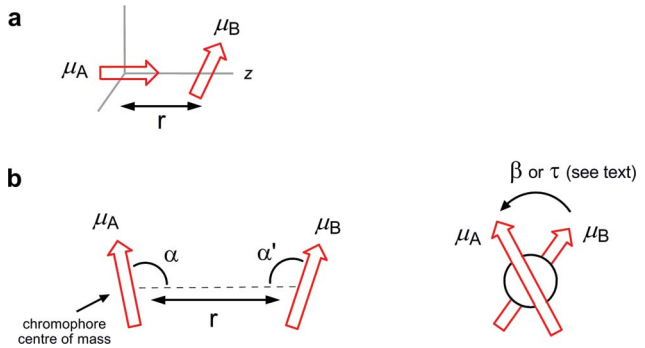

Fig. 3 Geometrical parameters used to define the orientation of two transition dipole moments.

The excitonic energy levels are found by evaluating these expressions. This requires the introduction of a coordinate system, which can be derived from a computational study or from geometrical parameters taken from structural data.

A variety of related expressions exist in the literature for estimating the energy gap between the two excitonic states.[4–6] These expressions depend on a particular choice of geometrical parameters. Eqn (4) naturally introduces an angle for each of the dot products: β is the angle between μ_A and μ_B if their centres of mass are superimposed, α is the angle between μ_A and $\hat{r}$, and α' is the angle between μ_B and $\hat{r}$, where $\hat{r}$ is the vector connecting the centres of gravity of the chromophores and r is the length of this vector (Fig. 3b). Eqn (4) then becomes Eqn (5):

$$J = \frac{\mu^2}{r^3}(\cos\beta - 3\cos\alpha\cos\alpha') \quad (5)$$

Alternatively, the *dihedral angle* (τ) between μ_A and μ_B along the vector $\hat{r}$may be more conveniently extracted from structural data and can be used in place of β. This introduces additional sine factors involving α and α' to give Eqn (6):

$$J = \frac{2\mu^2}{r^3}(\sin\alpha\sin\alpha'\cos\tau + 2\cos\alpha\cos\alpha') \quad (6)$$

From these equations, it is clear that the extent of exciton coupling between two chromophores is very sensitive to the relative orientation of their transition dipole moments. It is therefore crucial that the direction of the dipoles can be assigned with good precision. This usually relies on one of several methods:

- by careful analogy with well established systems;
- by theoretical methods (computational chemistry);
- experimentally, for example by measuring the linear dichroism of the chromophore in an oriented medium such as a crystal or a stretched film.[6]

In addition to the mutual orientation of the transition dipoles, the magnitude of exciton coupling is dependent on several other factors:

- It is strongest when the electronic transitions of the chromophores are degenerate (*e.g.*, when the chromophores are identical).

- Exciton coupling is proportional to the square of the magnitude of the transition dipole moment, μ. This can be rationalised by noting that dipoles that have a greater spatial extent (length) will have more significant interactions with nearby dipoles. Coupling is therefore rarely observed for weak electronic transitions such as d–d transitions of metal complexes.

- The chromophores must be close in space as the energy gap between the excitonic states is proportional to $1/r^3$, where r is the distance between the chromophores. Since the assembly of chromophoric ligands around a metal centre brings them into close proximity, exciton coupling effects are prominent in coordination compounds. *Intermolecular* exciton coupling may also be observed, for example when chromophoric complexes aggregate *via* noncovalent interactions, as is well known for H- and J- aggregates of organic dyes.

- Following on from the above point, the chromophores cannot be too close in space, however, as the model relies on the point-dipole approximation *i.e.*, that the distance between the chromophores is large relative to the length of the transition dipoles. Also, for the simple coupling model described here, there should be *negligible electron delocalisation* between the chromophores in the ground state of the array. This is usually a good approximation for chromophoric ligands that are coordinated to a metal centre, but it can break down for chromophores that are connected by bridges that allow a higher degree of conjugation.

By way of example, let us consider the case of hypothetical [ML_2] complexes of planar bidentate ligands that possess a transition dipole in the ligand plane and aligned along its long axis (Fig. 4).[7] The coordination geometry of such complexes can range from tetrahedral to square planar, as largely dictated by the identity of the metal ion. The dihedral angle (τ) between the transition dipoles of the two ligands can thus range from 0° to 90°. The angles α and α' (Fig. 3b) will be 90° for all equilibrium coordination geometries and the interchromophore distance, r, will again primarily be determined by the metal ion.

Two excitonic states will result from coupling of the chromophoric ligands, and Fig. 4 depicts the magnitude of the energy gap between the excitonic states as a function of τ. The energies of these states are shown relative to a comparable unperturbed chromophore. At $\tau = 90°$, Eqn (6) implies that there will be no splitting of the excited state. In terms of the vector model, this is due to the head-to-tail and head-to-head transition dipole combinations being indistinguishable. At $\tau = 0°$, the point

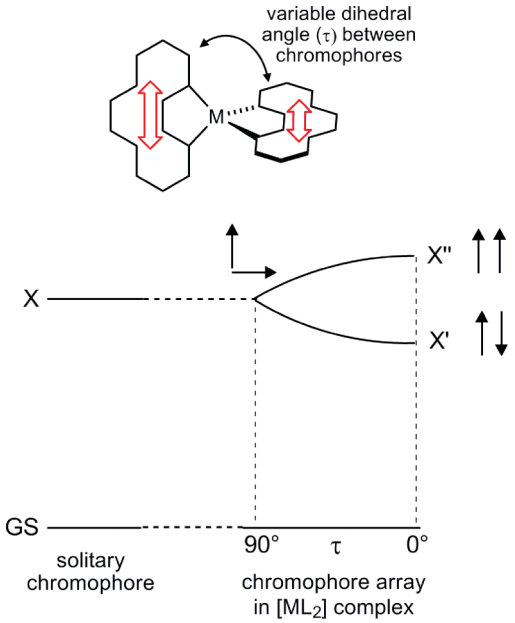

Fig. 4 Exciton coupling of two planar bidentate chromophoric ligands in $[ML_2]$ complexes leads to two excitonic states (X′ and X″). The energy gap between these states varies with cos τ, where τ is the dihedral angle between the transition dipole moments imposed by the metal centre.

of maximum exciton coupling is reached. This arrangement is identical to Fig. 2a, where electronic transitions to the X′ state are forbidden. Intermediate angles of τ are illuminating: two nondegenerate excited states exist and the energy gap between them varies with cos τ.

When τ = 90°, the intensities of the two exciton bands are equal to each other (and the bands are degenerate). As τ is progressively decreased from 90°, the intensities of the two absorption bands become more disparate, with the transition to the X″ state becoming increasingly more intense than that to the X′ state.[8]

This simple case illustrates the profound effect that the coordination geometry imposed by a metal ion can have on the nature of the electronic excited states of a complex *via* exciton coupling interactions. The effect of these interactions on experimentally measured electronic absorption and circular dichroism spectra of a range of transition metal complexes is outlined in the following two sections.

Exciton coupling effects in absorption spectra

Dipyrrinato ligands are chromophores in the visible wavelength region that can be viewed as 'half-porphyrin' chelates (Fig. 5). These ligands feature a low energy (~500 nm) absorption band that corresponds to a localised π–π* transition which is polarised in the chelate plane and parallel to a line connecting the N donor atoms. The transition dipole has a considerable magnitude (ε > 20,000 $M^{-1}cm^{-1}$ per ligand), which allows for strong exciton coupling. Thus, when multiple dipyrrin chromophores are brought into close proximity, for example by coordinating to the same metal ion, their π–π* absorption bands are often distinctly split. This is termed Davydov splitting. The clarity of this effect renders dipyrrin complexes ideal for illustrating the effects of exciton coupling in the following section. In principle, complexes of bipy or

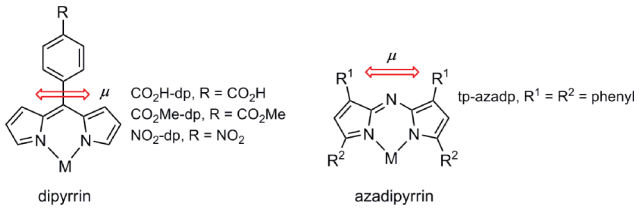

Fig. 5 The general structures of dipyrrin and azadipyrrin chelating ligands showing the orientation of the transition dipole moment of their lowest energy π–π* transition.

phen ligands could also serve as model systems, however, exciton coupling effects in their complexes are rather more subtle and serve to broaden their lowest energy π–π* absorption band and/or shift its position. Distinct splitting of this absorption band is not usually observed, and analysis is complicated by the presence of multiple closely-spaced transitions in the UV region.

Analysis of the exciton coupling in octahedral $[M(dipyrrinato)_3]$ complexes (Fig. 6) parallels the cases of $[M(bipy)_3]^{2+}$ and $[M(phen)_3]^{3+}$, which have been cogently summarised by Bosnich.[9] Under D_3 symmetry, the three localised transitions couple in three different ways. Two excitonic states are thus produced (X′ and X″), transitions to which are equally allowed. The higher energy (X″) state results from the "head-to-head" coupling of the dipoles ($\mu^1 + \mu^2 + \mu^3$) and has A symmetry, while the X′ excitonic state arises from two "head-to-tail" dipole coupling arrangements

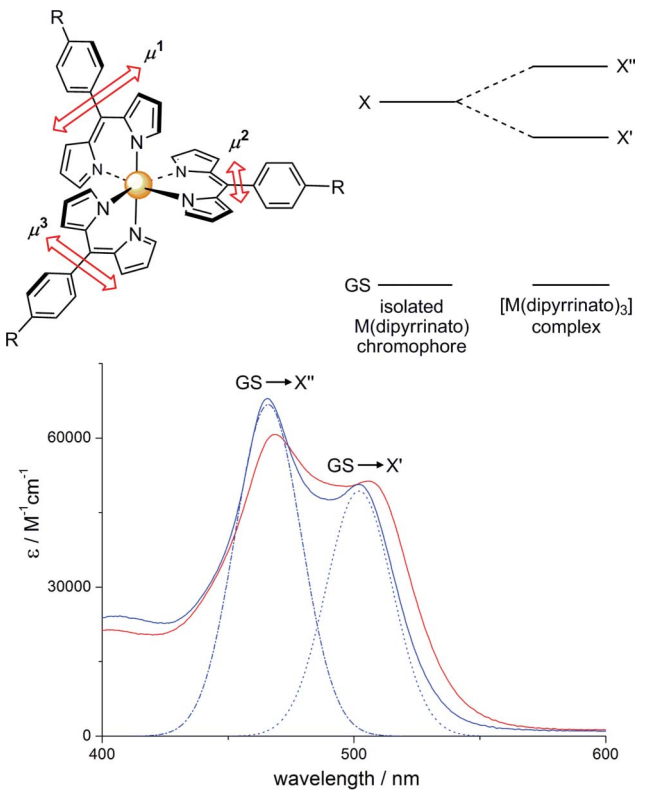

Fig. 6 The three dipyrrin chromophores in a D_3-symmetric octahedral $[M(dipyrrinato)_3]$ complex couple to give two excitonic states (X′ and X″). Transitions to these states are clearly observed in the electronic absorbance spectra of $[Co(CO_2H\text{-}dp)_3]$ (red line) and $[Rh(CO_2H\text{-}dp)_3]$ (blue line). The two major components of the observed spectrum of $[Rh(CO_2H\text{-}dp)_3]$ are shown in blue as dashed and dotted lines.

($2\mu^1 - \mu^2 - \mu^3$ and $\mu^2 - \mu^3$) and has E symmetry. Electronic transitions to the two excitonic states are apparent in the absorption spectra [M(CO_2H-dp)$_3$] complexes (M = Co(III), Rh(III)) in the guise of two distinct peaks around 470 and 505 nm (Fig. 6).[10,11] To emphasize the notion that the observed spectra result from the addition of two major components, these underlying transitions are presented in Fig. 6 for the Rh(III) complex. The delineation of exciton coupling effects in these complexes is aided by the fact that the low energy π–π* absorption bands of the dipyrrin ligands are both intense and energetically well-separated from other electronic transitions.

Splitting of excitonic states X′ and X″ is more pronounced in tris(dipyrrinato) complexes of Ga(III) and In(III) compared to the above examples.[12] On the other hand, exciton coupling appears to be weaker in [Fe(NO_2-dp)$_3$] and [Co(NO_2-dp)$_3$], where the transition to the X′ state appears as a shoulder on the higher energy transition.[13] Prominent exciton coupling features have also been noted in the spectra of heteroleptic dipyrrin/bipy complexes of ruthenium(II).[14]

Exciton coupling effects are also discernible in the absorption spectra of bis(dipyrrinato) complexes, many examples of which have been reported in the literature.[15,16] As outlined above (Fig. 4), the coordination geometry imposed by the metal in [M(dipyrrinato)$_2$] complexes will determine the impact of exciton coupling on their excited state energy levels. Absorption spectra of a selection of [M(CO_2Me-dp)$_2$] complexes are presented in Fig. 7. The square planar palladium(II) complex, in which $\tau \approx 0°$, exhibits one sharp absorption band centred at 483 nm. This band is blue-shifted with respect to complexes such as [Pd(CO_2Me-dp)(en)]$^+$ and [Pd(CO_2Me-dp)(dppe)]$^+$ (en = 1,2-diaminoethane, dppe = 1,2-bis(diphenylphosphino)ethane) in which the presence of a solitary dipyrrin chromophore obviates any exciton coupling.[10,17] The absorption maximum of these complexes is observed around 500 nm. For [Cu(CO_2Me-dp)$_2$], the absorption maxima appear at 470 nm and 502 nm. The lower intensity of the lower energy band is consistent with molecular structures determined by X-ray crystallography, which indicate that the angle between the dipyrrin chromophores is around 50–70°.[18,19] In [Zn(dipyrrinato)$_2$] complexes, the angle between the ligand planes is closer to 90°.[16]

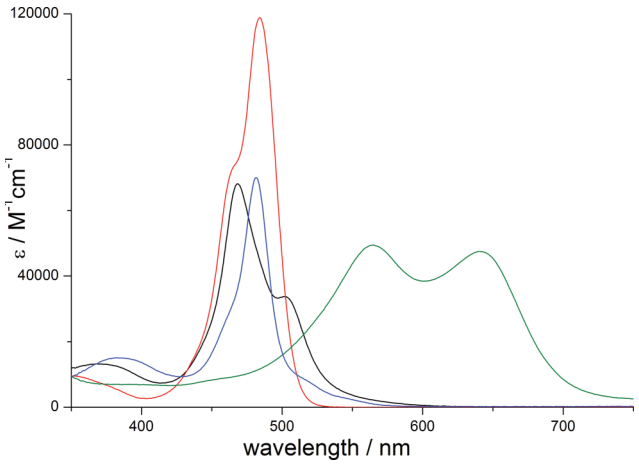

Fig. 7 Electronic absorption spectra of [Pd(CO_2Me-dp)$_2$] (blue), [Cu(CO_2Me-dp)$_2$] (black), [Zn(CO_2Me-dp)$_2$] (red) and [Cu(tp-azadp)$_2$] (green) recorded in solution at room temperature.

and the absorption maximum of [Zn(CO_2Me-dp)$_2$] is found at 484 nm. Exciton coupling in this complex is expected to be weak or non-existent; the high-energy shoulder on the main absorption band is reminiscent of [BF_2(dipyrrinato)] (bodipy) compounds and can probably be ascribed to vibronic coupling.

Azadipyrrinato complexes, [M(tp-azadp)$_2$], may also yield to a similar treatment. The Co(II), Ni(II), and Zn(II) complexes all have prominent shoulders on the red side of their intense π–π* absorption bands around 600 nm.[20] This is consistent with their X-ray crystal structures, which show that the angles between the chromophore planes are about 50°. [Cu(tp-azadp)$_2$] features peaks at 567 and 640 nm (Fig. 7). The extremely large energy gap between these peaks and their approximately equal intensities points to (i) very strong exciton coupling (consistent with the strong allowedness of the azadipyrrin transitions), and (ii) an angle between the ligand planes of close to 90° (see above). The X-ray crystal structure of [Cu(tp-azadp)$_2$] exhibits an angle of around 55° between the ligand planes.[20] At this geometry the absorption peaks would be expected to have considerably different intensities, which may imply that the exciton model does not actually hold for this complex. This may be a consequence of electronic overlap between the two ligands *i.e.*, the molecular orbitals of the complex may be distributed over *both* ligands rather than confined to one or the other. Similar observations have been made for porphyrin dimers.[21] We are currently tackling this anomaly using both Raman spectroscopy and TD-DFT calculations.

The exciton coupling model has illuminated the absorption spectra of many other chromophoric ligands. For example, a high degree of structural information on a series of M^{3+} complexes of a tris(acetylacetonate) ligand (**L**^{1}) was elucidated by the analysis of exciton coupling effects in their electronic absorption spectra (Fig. 8).[22] When the ligand wraps around these metal ions, the acac chromophores are brought into close proximity, which switches on exciton coupling. The effect is most pronounced for the π–π* transition around 260 nm, which is polarised across the acac unit. The [Al(**L**^{1})] and [Ga(**L**^{1})] complexes were observed to develop

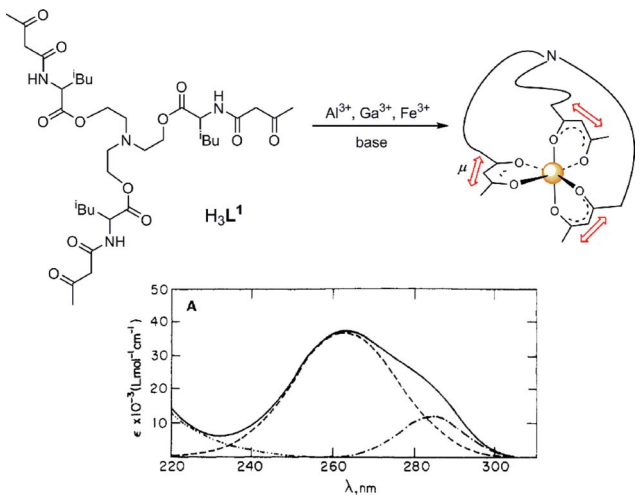

Fig. 8 Coordination of ligand **L**^{1} to a M^{3+} cation (M = Al, Ga, Fe) to give a [**ML**^{1}] complex (upper), and the absorption spectrum of [Al**L**^{1}] (lower). The experimental absorption spectrum (continuous line) can be deconvoluted into two Gaussian curves (dashed lines) that correspond to transitions to two excitonic states. Spectra reproduced from ref. 22. Copyright 1990 ACS.

a low-energy shoulder in their absorption spectra, which could be deconvoluted into individual transitions to the two expected excitonic states.

Meso-linked porphyrin arrays are probably the most well studied family of coordination compounds that display exciton coupling (Fig. 9).[23] Arrays of chromophores can be fabricated by the covalent tethering of multiple porphyrin subunits. Exciton coupling interactions between the subunits enables efficient energy transfer, also termed excited state "hopping" or Förster transfer. When the porphyrins are arranged in an extended 1-D array, this phenomenon enables them to act as optical wires.

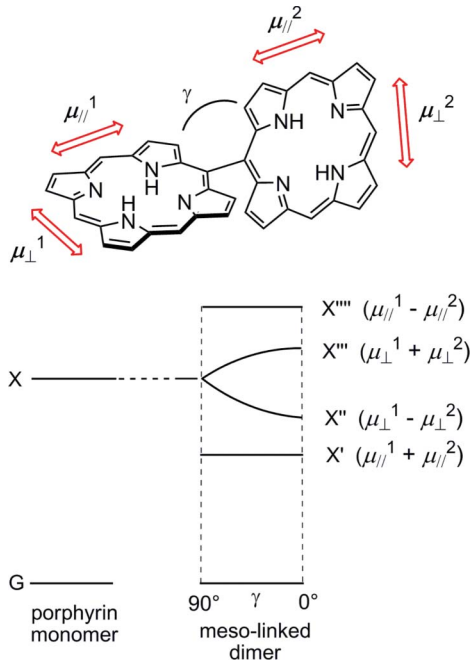

Fig. 9 Exciton coupling in *meso*-linked bis(porphyrins). The magnitude of the coupling between the perpendicular transition dipoles ($\mu_\perp^1$ and $\mu_\perp^2$) is dependent on the dihedral angle between the porphyrin planes (γ).

Two different types of exciton can be distinguished in such extended arrays of chromophores. If the excited electron and hole remain tightly bound and located on the same chromophore, the exciton is termed a Frenkel exciton.[24] This contrasts with Wannier–Mott excitons, where electron exchange between the chromophores allows the excited electron and hole to migrate away from one another.

With respect to the spectroscopic properties of porphyrin arrays, each porphyrin subunit features two transition dipole moments that lie in the porphyrin plane.[23] These are oriented either parallel ($\mu_{//}$) or perpendicular ($\mu_\perp$) to the transporphyrin bond (Fig. 9). These dipoles relate to nearly degenerate electronic transitions in porphyrin monomers and contribute to the Soret bands observed in their electronic absorption spectra.

With respect to *meso*-linked bis(porphyrins), the dihedral angle between the porphyrin planes (γ) is typically around 90°. In this conformation, $\mu_\perp^1$ and $\mu_\perp^2$ do not couple while $\mu_{//}^1$ and $\mu_{//}^2$ add and subtract to give two excitonic states (X′ and X′′′′). The net transition dipole for the X′′′′ state is zero, hence transitions to it are forbidden (see Fig. 2b). The upshot of this is that an absorption band is maintained at the position of the monomer Soret band and a second band appears at lower energy due to transitions to the X′ excitonic state.

Electronic interactions between the porphyrin subunits are enhanced when their orthogonality is broken (γ ≠ 90°) and the X″ and X‴ excitonic states become nondegenerate (Fig. 9). The situation now resembles that described above for two parallel transition dipoles with a variable dihedral angle. If an ensemble of bis(porphyrin) chromophores exist with a range of conformations (*i.e.* γ assumes a range of values), the high energy band will broaden.[21] If the relative conformation of the porphyrin rings is fixed, for example by tethering the porphyrins to one another, the transitions to the X″ and X‴ states are quite sharp,[25] and, for small values of γ, transitions to the X″ and X‴ states become distinct in the electronic absorption spectrum. The limits of the exciton coupling model have been explored in a *meso–meso* β–β doubly linked bis(porphyrin).[26]

Porphyrin chromophores have also been brought into close proximity by the reaction of pyridyl-substituted porphyrins with $[RuCl_2(dmso)_2(CO)_2]$ (Fig. 10).[27] This produces dinuclear metallacycles in which the two porphyrins are held in a fixed orientation. This orientation can be either 'slipped cofacial' or planar, depending on the attachment point of the pyridyl group. In the cofacial arrangement, the porphyrin Soret band was observed to be split by exciton coupling whereas the planar arrangement gives a single absorption band.

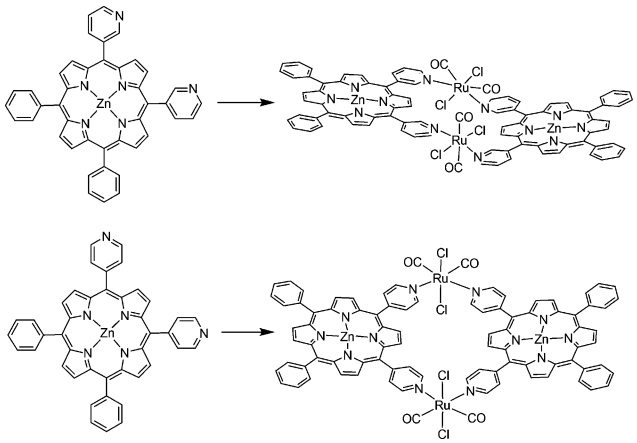

Fig. 10 Bis(porphyrin) metallacycles from the reaction of pyridyl-substituted porphyrins with $[RuCl_2(dmso)_2(CO)_2]$. The 3-pyridyl substituted porphyrin leads to a slipped cofacial arrangement of the chromophores (upper), while the 4-pyridyl substituted porphyrin leads to a planar arrangement (lower).

Splitting of the intense Q band of the phthalocyanine unit of a Ru(polypyridyl)-phthalocyanine dyad has been ascribed to exciton coupling between the Ru-terpyridine MLCT transition and the Q band of the Zn-phthalocyanine unit.[28] The Q band appears as two peaks around 704 and 673 nm. The effect of changes in molecular geometry, which alter the relative orientation of the transition dipoles, is highlighted by the fact that related complexes – in which the two chromophores are nonplanar – do not display exciton coupling.[29]

Electronic spectra of *noncovalent* porphyrin aggregates have also been successfully interpreted in the context of an exciton coupling model.[30] Both steady-state properties and singlet and triplet

energy transfer dynamics of the array of chlorophyll molecules in the light-harvesting (LHC) complex II of photosystem II depend heavily on interactions between these chromophores.[31,32] The importance of excitons in LHC II and other nanoscale systems, such as quantum dots, conjugated polymers, and carbon nanotubes has recently been reviewed by Scholes and Rumbles.[33]

Exciton coupling effect in circular dichroism (CD) spectra

Background

Circular dichroism (CD) spectroscopy measures the difference between the absorption of right- and left-circularly polarised light. Nonracemic samples of chiral compounds can give rise to peaks (also termed Cotton effects) in CD spectra in wavelength regions where they have an electronic transition.

If two identical chromophores are located in close spatial proximity and have a chiral disposition, *i.e.* they are not related by an improper axis of symmetry, exciton coupling can produce bisignate curves, termed *exciton couplets*, in their CD spectra.[6,34] These couplets arise because the electronic transitions to the excitonic states (X′ and X″) are excited to differing degrees by right- and left-circularly polarised light. Fig. 11 shows how each transition gives rise to Cotton effects of mutually opposite sign (blue and red curves), the summation of which produces a bisignate spectrum (black curve) that is characteristic of exciton coupling. The exciton couplet in Fig. 11 has a positive amplitude at lower energy hence it is termed a positive exciton couplet. The mirror image of this chromophore array will display a mirror-image CD signal *i.e.*, a negative exciton couplet.

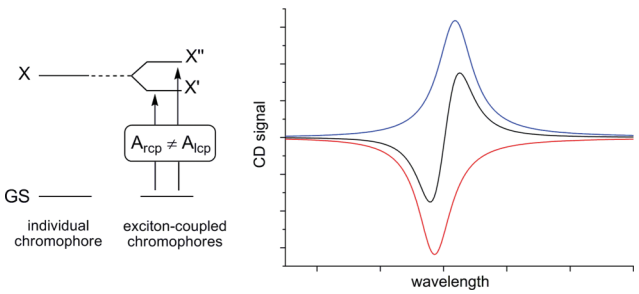

Fig. 11 Transitions to excitonic states of a chiral array of chromophores are excited to differing extents by right- and left-circularly polarised light ($A_{rcp} \neq A_{lcp}$). This gives rise to an exciton couplet as shown in the hypothetical CD spectrum (black curve), which results from the summation of positive (blue curve) and negative (red curve) Cotton effects.

The sign and magnitude of the Cotton effects that comprise an exciton couplet are defined by rotational strengths (R^A and R^B), the CD equivalent of oscillator strengths in linear absorption spectroscopy, which are given by Eqn (7):[6]

$$R^{A/B} = \pm\frac{E\mu^2 r}{4\hbar}(\sin\alpha\sin\gamma\sin\tau) \quad (7)$$

Here τ is defined as the *anticlockwise* dihedral angle between the two dipole moments, as illustrated in Fig. 3b, and E is the energy of the transition from the ground state to the unperturbed excited state (X). With reference to Eqn (6), the energies at which R^A and R^B occur, E^A and E^B, are given by Eqn (8):[6]

$$E^{A/B} = E \pm \frac{\mu^2}{r^3}(\sin\alpha\sin\gamma\cos\tau + 2\cos\alpha\cos\gamma) \quad (8)$$

From Eqn (7), we can note that the rotational strengths depend on several factors:

- Their magnitude is proportional to the square of the oscillator strengths of the electronic transitions in the isolated chromophores. Although the magnitude of the rotational strengths is maximised when α, α′, and τ are all 90°, they become degenerate with this orientation and thus cancel. This is consistent with this orientation representing an *achiral* array.
- The relative orientations of the chromophores. Inverting the chirality of a chromophore array involves changing τ to 360 − τ, hence R^A and R^B will switch sign and the exciton couplet will change phase. However, an inversion of an exciton couplet does not necessarily mean that that the absolute configuration of the chromophore array has changed *e.g.*, the energy ordering of R^A and R^B will switch upon going from α = α′ = 50° to α = α′ = 60° for τ = 160°.[5]
- The distance between the chromophores. Note that, at face value, Eqn (7) predicts that rotational strengths will increase linearly with the distance between the chromophores. However, as the energetic separation of R^A and R^B falls off as a function of r^{-3} (Eqn (8)), the CD signal is effectively proportional to r^{-2}.[6,35]

The interpretation of CD spectra with the exciton coupling model is most reliable when the transition of interest is energetically well separated from, and not mixed with, other electronic transitions. In this case, the exciton couplet will not be obscured by other spectral bands and thus easily identifiable. The wavelength corresponding to the zero point of an exciton couplet is centred on the absorption maximum of an unperturbed chromophore, and the areas under the positive and negative Cotton effects are equal.

Exciton coupling in the CD spectra of mononuclear complexes

One of the most powerful applications of the analysis of exciton coupling in CD spectra is the assignment of the absolute configuration of the dominant enantiomer in a nonracemic mixture. This is a *nonempirical* method based on Eqn (7) and Eqn (8). The angles required for input into these equations can be obtained from X-ray crystal structures or computational models.

This relationship between the sign of an exciton couplet and absolute configuration is exemplified for octahedral complexes with two or more bidentate ligands that have transition dipoles aligned across the chelate ring, for example bipy, phen, dipyrrins, and acetylacetonate (acac). In these complexes, α and α′ are around 105° and τ is around 300° for the Λ absolute configuration. Thus, R^A is negative and $E^A > E^B$, which corresponds to a positive exciton couplet (Fig. 12). The following general rule relates the sign of the exciton couplet with the absolute configuration of the metal centre for this family of octahedral tris(bidentate) complexes:

The Δ absolute configuration at the metal centre will give rise to an exciton couplet with a negative peak at lower energy and a positive peak at higher energy and vice-versa for a complex with Λ absolute configuration.

Excellent early reviews of the application of the exciton coupling model to the assignment of the absolute configuration of

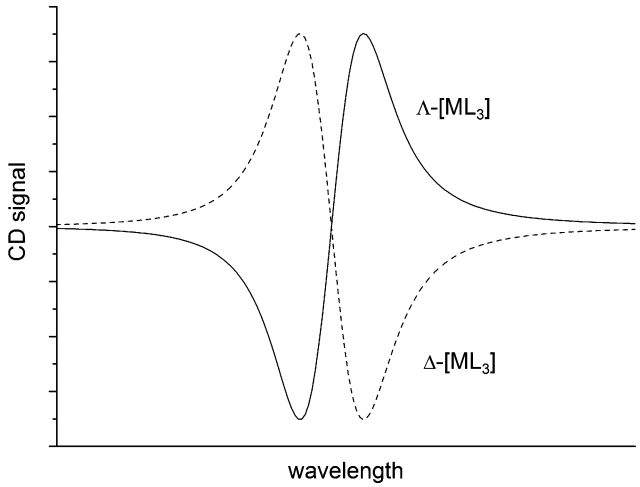

Fig. 12 The Δ absolute configuration of an octahedral $[ML_3]$ complexes with ligands such as phen, bipy, dipyrrinato and acac gives rise to a negative exciton couplet (dotted line), and the Λ absolute configuration produces a positive exciton couplet (continuous line).

octahedral bipy, phen and acac complexes were provided by Mason[36] and Bosnich.[9] Ziegler and von Zelewsky subsequently reviewed its application to 'chiragen' complexes of chiral bipy and phen ligands.[5] Autschbach and Ziegler have calculated the CD spectra[37] of octahedral $[M(phen)_3]^{n+}$ [38] and $[M(bipy)_3]^{n+}$ [39] complexes using DFT, and have outlined how their computational results relate to the exciton coupling model.[39]

In the following section we present a selection of recent examples of the analysis of exciton coupling features in the CD spectra of transition metal complexes to highlight the range of chromophores to which the model can be applied.

The carboxyl 'tags' on the complex $[Co(CO_2H\text{-}dp)_3]$ allow it to be resolved by classical methods involving the selective precipitation of a diastereoisomeric salt.[11] Cinchonidine proved to be an effective partner for $[Co(CO_2H\text{-}dp)_3]$, and both enantiomers can be obtained with an enantiomeric excess (e.e.) of 100%. The CD spectra of Δ- and Λ-$[Co(CO_2H\text{-}dp)_3]$ (Fig. 13) show prominent exciton couplets in the visible region and, as expected, the two spectra are mirror images of one another. The sign of the exciton

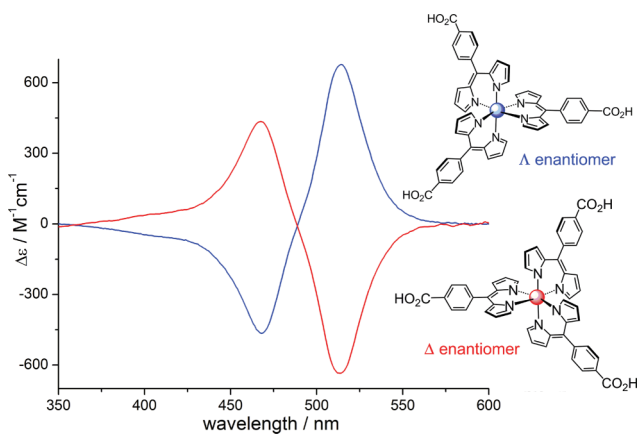

Fig. 13 CD spectra of Δ-$[Co(CO_2H\text{-}dp)_3]$ (blue line) and Λ-$[Co(CO_2H\text{-}dp)_3]$ measured in DMSO solution.[11]

couplet allowed assignment of the absolute configuration of each sample, which was also supported by X-ray crystallography.

Chiral, enantiopure ligands can be put to good effect for the stereoselective synthesis of chiral metal complexes.[40] In this way, the absolute configuration of a metal can be 'predetermined' by the chirality of the ligand. The analysis of exciton coupling in the CD spectra of these complexes provides a straightforward method for the assignment of the absolute configuration of the metal centre. For example, enantiopure L-valine groups appended to a bipy framework produce $[M(\mathbf{L}^2)_3]^{2+}$ ($M = Co^{II}$, Fe^{II}) complexes with complete diastereoselectivity (as adjudged by ^1H NMR spectroscopy).[41] A prominent exciton couplet centred around 300 nm is observed in the CD spectra of both complexes (Fig. 14). The sign of the exciton couplet allowed the metal centres to be assigned the Δ absolute configuration.

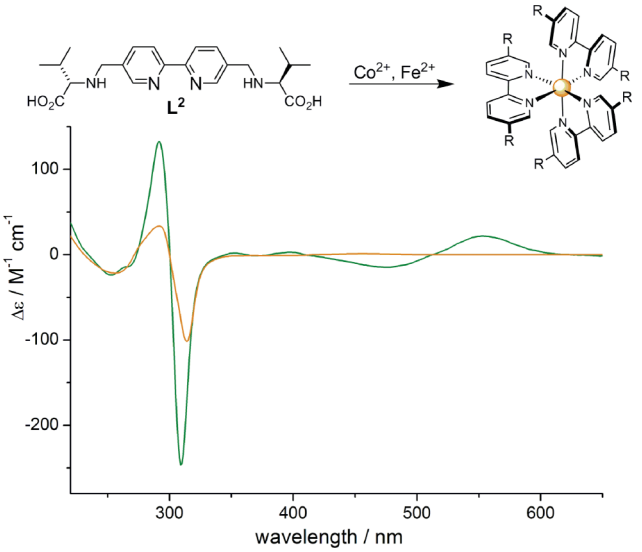

Fig. 14 Ligand $\mathbf{L}^2$ coordinates to Co(II) and Fe(II) to give Δ-$[M(\mathbf{L}^2)_3]^{2+}$ complexes with complete diastereoselectivity. Analysis of the exciton couplet in the CD spectrum around 300 nm allowed the absolute configuration of the metal centre to be assigned (orange = Co(II), green = Fe(II)). Additional bands of relatively high intensity are also observed in the visible wavelength region of the Fe(II) complex, which are associated with MLCT transitions.

Scott *et al.* have recently reported that simple chiral iminopyridine ligands ($\mathbf{L}^3$) chelate to Fe(II) with high diastereoselectivity (Fig. 15).[42] Only *fac* isomers are observed, and the *R* absolute configuration of the ligand enforces the Δ absolute configuration of the metal. This conclusion was arrived at using X-ray crystallography, however prominent exciton couplets centred around 290 nm are observed in the CD spectra of these complexes. There is a π–π transition of the conjugated pyridyl-imine chromophore in this region whose transition dipole is aligned across the chelate (akin to bipy and phen).[43] The above rule relating the absolute configuration of the metal centre to the sign of the exciton couplet is thus also applicable to this family of complexes, leading to stereochemical assignments that agree with the crystallographic results.

Canary's group has investigated complexes of substituted methionine ligands whose CD spectra show interesting responses to external stimuli. For example, reduction of the copper(II) centre

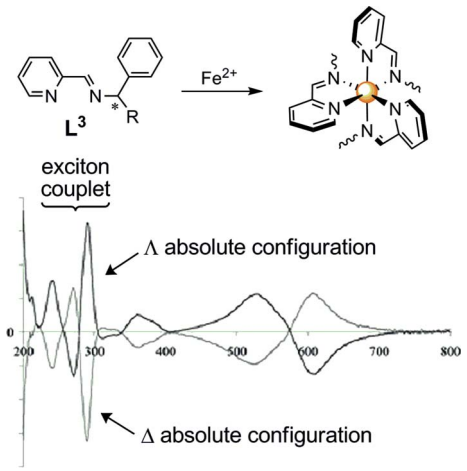

Fig. 15 Chiral, enantiopure imino-pyridine ligands chelate to Fe(II) to give $[Fe(\mathbf{L}^3)_3]^{2+}$ complexes with high diastereoselectivity.[42] A prominent exciton couplet around 290 nm is observed in the CD spectra of the complexes where R = CH_3. This can be used to assign the absolute configuration of the metal centre. Spectra reproduced from ref. 42 Copyright 2009 The Royal Society of Chemistry (RSC).

in the complex shown in Fig. 16 induces a reorganisation of the coordination sphere that is coupled to a change in the relative orientation of two quinoline chromophores.[44] This inverts the phase of the observed exciton couplet. Exciton couplets in the CD spectra of complexes of similar ligands derived from chiral amines are also redox-switchable.[45] This phenomenon has been developed as a method for determining the absolute configurations and enantiomeric excess of amino acids.[46]

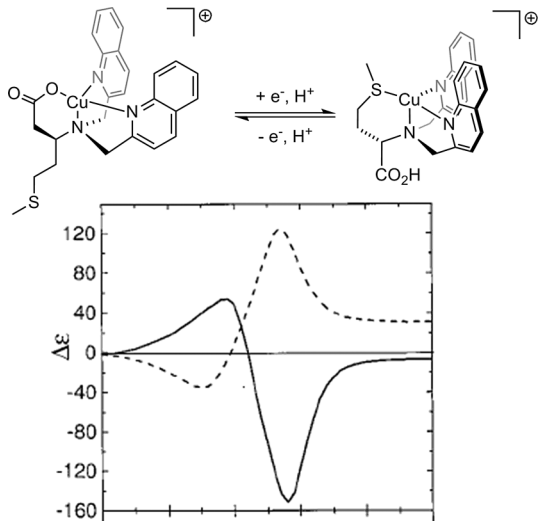

Fig. 16 Reduction of a copper(II) complex of a quinolyl-substituted methionine ligand is coupled to a change in the relative orientation of the two quinolyl chromophores.[44] This inverts the exciton couplet observed in the CD spectrum: the full line corresponds to the copper(II) complex, while the dashed line corresponds to the copper(I) complex. Spectra reproduced with permission from ref. 44 Copyright 2000 AAAS.

A positive exciton couplet was observed around 265 nm following the diastereoselective coordination of an enantiopure tris(quinolinol) peptide ligand ($\mathbf{L}^4$) to a range of M^{3+} cations (Fig. 17).[47] Presuming that the transition dipole moment of

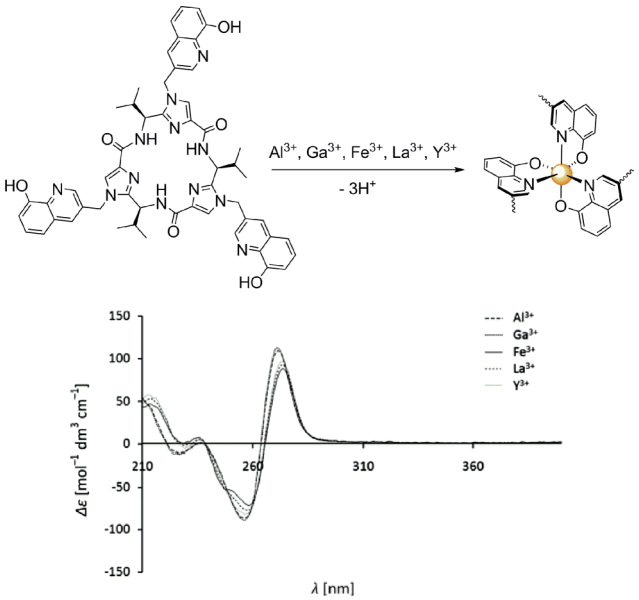

Fig. 17 Ligand $\mathbf{L}^4$ coordinates to a range of M^{3+} cations with complete diastereoselectivity. The absolute configuration of the metal centre can be assigned as Λ on the basis of the positive exciton couplet around 265 nm. Spectra reproduced with permission from ref. 47 Copyright 2009 Wiley-VCH.

quinolinolate chelates lies in the ligand plane and is oriented roughly parallel to the vector connecting the N and O donor atoms, the CD spectra clearly imply that the absolute configuration of these complexes is Λ. The reported computational results are in accord with this analysis.

In selected other examples, exciton coupling between the benzimidazole chromophores in an osmium(II) tris(benzimidazolate) complex, which had been resolved on an ion exchange resin with a chiral eluent, was used to assign its absolute configuration.[48] Elsewhere, distinct exciton couplets in the UV region, which arise from π–π* transitions of catecholate ligands, were used to assign the absolute configuration of tetranuclear cage complexes.[49] Exciton coupling between chiral arrays of porphyrins has also been intensively studied in the context of sensors for chiral guests.[50] Further, azomethene chromophores in chiral cyclohexanediamine-based Schiff base ligands interact to give prominent exciton couplets, from which the absolute configuration of a range of complexes could be determined.[51]

Internuclear exciton coupling

Our discussion up to this point has concentrated on exciton interactions between chromophores that are coordinated to the same metal centre. What happens between chromophores coordinated to different metal centres? It can be noted the role of the metal is purely structural, *i.e.*, it brings the chromophores close in space, but, if the exciton coupling model is to remain valid, it does not act as a conduit for communication between the chromophores. Thus, provided that they are close enough in space, and are appropriately aligned (Eqn (7) & Eqn (8)), coupling between chromophores coordinated to different metal centres can be expected to be significant.

This was first recognised in practise for the dinuclear cobalt(II) complex of **L**[5] presented in Fig. 18, which provides a striking example of what we termed *internuclear exciton coupling*.[43] X-ray crystallography provided the absolute configurations of the metal centres of this complex (both Λ), and showed that the pyridylimine chromophores chelated to different metal centres are actually held relatively close to one another. This switches on internuclear exciton coupling interactions *i.e.*, exciton coupling interactions between chromophores located on different metal centres. These interactions contribute strongly to the observed CD spectrum, and actually outweigh the 'intranuclear' exciton coupling mode. A negative exciton couplet is observed, rather than the positive couplet that would have been predicted by considering the metal centres in isolation.

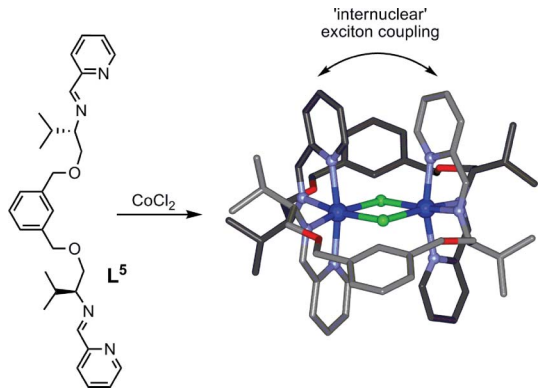

Fig. 18 Reaction of a enantiopure bis(bidentate) pyridyl-imine ligand derived from L-valinol (**L**[5]) with $CoCl_2$ produces a dinuclear complex with a $Co_2(\mu_2\text{-}Cl)_2$ core. Exciton coupling between chromophores located on different metal centre (*internuclear* exciton coupling) dominates the observed CD spectrum.

Following the realisation that internuclear exciton effects could have such a pronounced effect on observed CD spectra, the spectra of other metallosupramolecular assemblies were analysed within this framework.[52] Many of these arrays are constructed using phen- or bipy-based ligands, which are amenable to analysis as their lowest energy π–π* transitions have well defined transition dipole moments. It was found that a significant number of reported supramolecular assemblies give rise to CD spectra that have anomalously low intensities. A striking example is the comparison of the amplitudes of the CD spectra (defined as $\Delta\varepsilon^1 - \Delta\varepsilon^2$, where $\Delta\varepsilon^1$ is the intensity of the lower energy band of the exciton couplet and $\Delta\varepsilon^2$ is the intensity of the higher energy band) of Λ-$[Ru(bipy)_2(bpm)]^{2+}$ and Λ,Λ-$[(phen)_2Ru(bpm)Ru(phen)_2]^{4+}$ (Fig. 19) in the region of the lowest energy π–π* transition of the phen chromophores. The amplitude of the *mononuclear* complex is 386 $M^{-1}cm^{-1}$, while the value for the *dinuclear* complex is 145 $M^{-1}cm^{-1}$. This anomaly can be resolved by taking into account internuclear exciton coupling effects (though there are minor complications that arise from the coupling of the bpm and phen chromophores, which are nondegenerate). The intensities of a range of other polynuclear complexes can be similarly accounted for.[52]

The analysis of internuclear exciton coupling effects has subsequently proved fruitful in the analysis of the CD spectra of other polynuclear complexes. For example, a segmental benz-

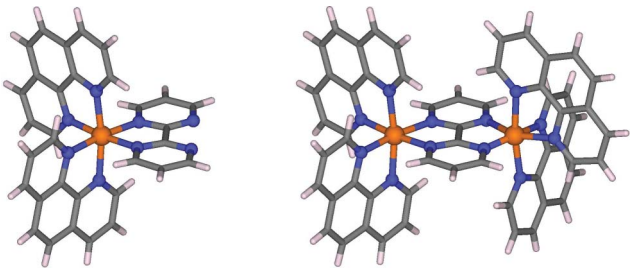

Fig. 19 Structures of Λ-$[Ru(bipy)_2(bpm)]^{2+}$ (left) and Λ,Λ-$[(bipy)_2\text{-}Ru(bpm)Ru(bipy)_2]^{4+}$ (right). Bpm = 2,2′-bipyrimidine.

imidazole/amidobenzimidazole ligand chelates to Cr(III) *via* its benzimidazole groups to give a *fac*-$[Cr(L)_3]^{3+}$ complex, which can be resolved into its two enantiomers (Fig. 20).[53] Titration of Eu(III) into a solution of this complex produces the heterobimetallic helicate Λ,Λ-$[EuCr(L)_3]^{6+}$ by coordination of the Eu(III) ions to the amidobenzimidazole segments. This process can be monitored by CD spectroscopy, which displays significant changes in the UV region. Notably, the exciton couplet centred around 325 nm is seen to invert (Fig. 20). This can be primarily ascribed to internuclear exciton coupling.[54]

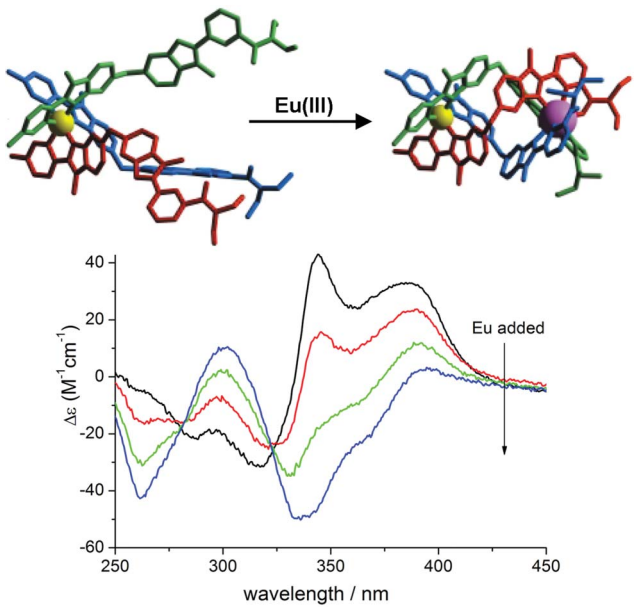

Fig. 20 The titration of Eu(III) ions into a solution of a resolved Cr(III) complex leads to the formation of the heterobimetallic helicate. The CD spectrum undergoes significant changes in the UV region, which can be rationalised on the basis of internuclear exciton coupling.

Elsewhere, an interesting case of exciton coupling has been reported for a *single stranded* chiral di(rhenium(I)) quaterpyridine helicate, in which the coordination of a sole di-imine chromophore to each metal rules out the possibility of intranuclear exciton coupling.[55] The observed CD signals can be ascribed solely to internuclear exciton coupling. The same authors have reported a double stranded dinuclear copper(I) helicate of a related tetradentate pyridylthiazole ligand.[56] Various exciton interactions are possible between the four pyridylthiazole chromophores, which combined to give a rather complicated experimental CD

spectrum. A similar analysis can be made for copper(I) and silver(I) dinuclear double stranded helicates of chiral bis-5,6-pinene bipyridyl ligands[57] as well as polynuclear lanthanide complexes of related ligands.[58] The anomalously weak and complicated CD spectra of homochiral multinuclear ruthenium(II) complexes of oligomeric bibenzimidazole and bipyridyl ligands can also probably be ascribed to the multitude of possible internuclear exciton coupling interactions.[59] It is possible that the CD spectra of many other complexes that have appeared in the literature may also be fruitfully interpreted by considering internuclear exciton coupling interactions.[60]

Summary

Exciton coupling can give rise to prominent effects in the absorption and circular dichroism spectra of transition metal complexes with chromophoric ligands. One common effect is to broaden the absorption window of the complex, thus is represents a potential strategy for improving the light-harvesting efficiency of transition metal dyes employed as solar cell sensitisers or photocatalysts. Here, there are parallels with LHC II, in which an array of interacting chromophores absorbs solar radiation much more effectively than the same number of isolated chromophores.[32]

With respect to CD spectroscopy, the analysis of exciton coupling effects provides a non-empirical method for the determination of the absolute configuration of the metal centre. The method can be extended to polynuclear complexes, as often encountered in supramolecular chemistry, but requires the consideration of long-range 'internuclear' exciton coupling in addition to conventional shorter range interactions.

Notes and references

1 M. Kasha, *Rev. Mod. Phys.*, 1959, **31**, 162–169; M. Kasha, in *Physical Processes in Radiation Biology*, Academic Press, New York, Editon edn, 1964, pp. 17–19.
2 M. Kasha, H. R. Rawls and M. A. El-Bayoumi, *Pure Appl. Chem.*, 1965, **11**, 371–392.
3 J. A. Schellman, *Acc. Chem. Res.*, 1968, **1**, 144–151.
4 J. Seibt, P. Marquetand, V. Engel, Z. Chen, V. Dehm and F. Wuerthner, *Chem. Phys.*, 2006, **328**, 354–362; G. Palmer and M. Degli Esposti, *Biochemistry*, 1994, **33**, 176–185.
5 M. Ziegler and A. von Zelewsky, *Coord. Chem. Rev.*, 1998, **177**, 257–300.
6 A. Rodger and B. Norden, *Circular Dichroism and Linear Dichroism*, Oxford University Press, Oxford, 1997.
7 Related examples for dimers of organic perylene bisimide chromophores can be found in an excellent recent publication: J. Seibt, P. Marquetand, V. Engel, Z. Chen, V. Dehm and F. Wuerthner, *Chem. Phys.*, 2006, **328**, 354–362.
8 N. Berova, D. Gargiulo, F. Derguini, K. Nakanishi and N. Harada, *J. Am. Chem. Soc.*, 1993, **115**, 4769–4775.
9 B. Bosnich, *Acc. Chem. Res.*, 1969, **2**, 266–273.
10 J. D. Hall, T. M. McLean, S. J. Smalley, M. R. Waterland and S. G. Telfer, *Dalton Trans.*, 2010, **39**, 437–445.
11 S. G. Telfer and J. D. Wuest, *Chem. Commun.*, 2007, 3166–3168.
12 V. S. Thoi, J. R. Stork, D. Magde and S. M. Cohen, *Inorg. Chem.*, 2006, **45**, 10688–10697.
13 C. Bruckner, Y. Zhang, S. J. Rettig and D. Dolphin, *Inorg. Chim. Acta*, 1997, **263**, 279–286.
14 S. J. Smalley, M. R. Waterland and S. G. Telfer, *Inorg. Chem.*, 2009, **48**, 13–15.
15 T. E. Wood and A. Thompson, *Chem. Rev.*, 2007, **107**, 1831–1861.
16 L. Yu, K. Muthukumaran, I. V. Sazanovich, C. Kirmaier, E. Hindin, J. R. Diers, P. D. Boyle, D. F. Bocian, D. Holten and J. S. Lindsey, *Inorg. Chem.*, 2003, **42**, 6629–6647.
17 C. Bronner, S. A. Baudron, M. W. Hosseini, C. A. Strassert, A. Guenet and L. De Cola, *Dalton Trans.*, 2010, **39**, 180–184.
18 S. R. Halper and S. M. Cohen, *Chem.–Eur. J.*, 2003, **9**, 4661–4669.
19 T. M. McLean and S. G. Telfer. Unpublished observations.
20 A. Palma, J. F. Gallagher, H. Mueller-Bunz, J. Wolowska, E. J. L. McInnes and D. F. O'Shea, *Dalton Trans.*, 2009, 273–279.
21 H. L. Anderson, *Inorg. Chem.*, 1994, **33**, 972–981.
22 Y. Tor, A. Shanzer and A. Scherz, *Inorg. Chem.*, 1990, **29**, 4096–4099.
23 D. Kim and A. Osuka, *Acc. Chem. Res.*, 2004, **37**, 735–745; K. Susumu, T. Shimidzu, K. Tanaka and H. Segawa, *Tetrahedron Lett.*, 1996, **37**, 8399–8402; A. Osuka and H. Shimidzu, *Angew. Chem., Int. Ed. Engl.*, 1997, **36**, 135–137.
24 J. J. Piet, P. N. Taylor, B. R. Wegewijs, H. L. Anderson, A. Osuka and J. M. Warman, *J. Phys. Chem. B*, 2001, **105**, 97–104; V. May and O. Kuhn, *Charge and Energy Transfer Dynamics in Molecular Systems*, 2nd edn, Wiley-VCH, Weinheim, 2004.
25 N. Yoshida, T. Ishizuka, A. Osuka, D. H. Jeong, H. S. Cho, D. Kim, Y. Matsuzaki, A. Nogami and K. Tanaka, *Chem.–Eur. J.*, 2003, **9**, 58–75.
26 A. Muranaka, Y. Asano, A. Tsuda, A. Osuka and N. Kobayashi, *ChemPhysChem*, 2006, **7**, 1235–1240.
27 E. Iengo, E. Zangrando, M. Bellini, E. Alessio, A. Prodi, C. Chiorboli and F. Scandola, *Inorg. Chem.*, 2005, **44**, 9752–9762.
28 F. Odobel and H. Zabri, *Inorg. Chem.*, 2005, **44**, 5600–5611.
29 M. Kimura, T. Hamakawa, K. Hanabusa, H. Shirai and N. Kobayashi, *Inorg. Chem.*, 2001, **40**, 4775–4779.
30 J. M. Ribo, J. M. Bofill, J. Crusats and R. Rubires, *Chem.–Eur. J.*, 2001, **7**, 2733–2737; J. Zimmermann, U. Siggel, J.-H. Fuhrhop and B. Roeder, *J. Phys. Chem. B*, 2003, **107**, 6019–6021.
31 H. van Amerongen and R. van Grondelle, *J. Phys. Chem. B*, 2001, **105**, 604–617.
32 H. Van Amerongen, L. Valkunas and R. van Grondelle, *Photosynthetic Excitons*, World Scientific, Singapore, 2000.
33 G. D. Scholes and G. Rumbles, *Nat. Mater.*, 2006, **5**, 683–696.
34 N. Harada and K. Nakanishi, *Circular Dichroic Spectroscopy - Exciton Coupling in Organic Stereochemistry*, University Science Books, Mill Valley, CA, 1983J. Gawronski and P. Skowronek, in *Chiral Analysis*, ed. K. W. Busch and M. A. Busch, Elsevier, Amsterdam, Editon edn, 2006, pp. 397–459.
35 N. Harada, S.-M. L. Chen and K. Nakanishi, *J. Am. Chem. Soc.*, 1975, **97**, 5345–5352.
36 S. F. Mason, *Inorg. Chim. Acta, Rev.*, 1968, **2**, 89–109.
37 J. Autschbach, *Chirality*, 2009, **21**, E116–E152.
38 B. Le Guennic, W. Hieringer, A. Goerling and J. Autschbach, *J. Phys. Chem. A*, 2005, **109**, 4836–4846.
39 J. Fan, J. Autschbach and T. Ziegler, *Inorg. Chem.*, 2010, **49**, 1355–1362.
40 U. Knof and A. von Zelewsky, *Angew. Chem., Int. Ed.*, 1999, **38**, 302–322.
41 S. G. Telfer, G. Bernardinelli and A. F. Williams, *Chem. Commun.*, 2001, 1498–1499; S. G. Telfer, G. Bernardinelli and A. F. Williams, *Dalton Trans.*, **2003**, 435–440.
42 S. E. Howson, L. E. N. Allan, N. P. Chmel, G. J. Clarkson, R. van Gorkum and P. Scott, *Chem. Commun.*, 2009, 1727–1729.
43 S. G. Telfer, R. Kuroda and T. Sato, *Chem. Commun.*, 2003, 1064–1065.
44 S. Zahn and J. W. Canary, *Science*, 2000, **288**, 1404–1407.
45 S. Zahn and J. W. Canary, *J. Am. Chem. Soc.*, 2002, **124**, 9204–9211.
46 A. E. Holmes, S. Zahn and J. W. Canary, *Chirality*, 2002, **14**, 471–477.
47 E. Ziegler and G. Haberhauer, *Eur. J. Org. Chem.*, 2009, 3432–3438.
48 T. Riis-Johannessen, N. Dupont, G. Canard, G. Bernardinelli, A. Hauser and C. Piguet, *Dalton Trans.*, 2008, 3661–3677.
49 A. V. Davis, D. Fiedler, M. Ziegler, A. Terpin and K. N. Raymond, *J. Am. Chem. Soc.*, 2007, **129**, 15354–15363.
50 V. V. Borovkov, G. A. Hembury and Y. Inoue, *Acc. Chem. Res.*, 2004, **37**, 449–459; G. A. Hembury, V. V. Borovkov and Y. Inoue, *Chem. Rev.*, 2008, **108**, 1–73.
51 E. Szłyk, M. Barwiołek, R. Kruszynski and T. J. Bartczak, *Inorg. Chim. Acta*, 2005, **358**, 3642–3652; E. Szlyk, A. Surdykowski, M. Barwiolek and E. Larsen, *Polyhedron*, 2002, **21**, 2711–2717.
52 S. G. Telfer, N. Tajima and R. Kuroda, *J. Am. Chem. Soc.*, 2004, **126**, 1408–1418.
53 M. Cantuel, G. Bernardinelli, G. Muller, J. P. Riehl and C. Piguet, *Inorg. Chem.*, 2004, **43**, 1840–1849.
54 S. G. Telfer, N. Tajima, R. Kuroda, M. Cantuel and C. Piguet, *Inorg. Chem.*, 2004, **43**, 5302–5310.
55 H.-L. Yeung, W.-Y. Wong, C.-Y. Wong and H.-L. Kwong, *Inorg. Chem. Comm.*, 2009, **48**, 4108–4117.

56 C.-S. Tsang, H.-L. Yeung, W.-T. Wong and H.-L. Kwong, *Chem. Commun.*, 2009, 1999–2001.
57 L.-E. Perret-Aebi, A. von Zelewsky and A. Neels, *New J. Chem.*, 2009, **33**, 462–465.
58 O. Mamula, M. Lama, S. G. Telfer, A. Nakamura, R. Kuroda, H. Stoeckli-Evans and R. Scopelitti, *Angew. Chem., Int. Ed.*, 2005, **44**, 2527–2531.
59 J. Yin and R. L. Elsenbaumer, *Inorg. Chem.*, 2007, **46**, 6891–6901.
60 C. R. K. Glasson, G. V. Meehan, J. K. Clegg, L. F. Lindoy, J. A. Smith, F. R. Keene and C. Motti, *Chem.–Eur. J.*, 2008, **14**, 10535–10538; M. Hutin, C. J. Cramer, L. Gagliardi, A. R. M. Shahi, G. Bernardinelli, R. Cerny and J. R. Nitschke, *J. Am. Chem. Soc.*, 2007, **129**, 8774–8780; B. Quinodoz, G. Labat, H. Stoeckli-Evans and A. von Zelewsky, *Inorg. Chem.*, 2004, **43**, 7994–8004.

